Investigation of Path Loss in a Complex Building Environment Using USRP and GNU Radio

Akinyele A. Itamakinde[1,*], Temitayo O. Ejidokun[1], Babatunde S. Adejumobi[1], Thokozani Shongwe[2], Emmanuel Adetiba[3,4], and Israel Esan Owolabi[1]

[1] Department of Electrical, Electronics and Computer Engineering, Afe Babalola University, Ado-Ekiti, Nigeria
[2] Department of Electrical and Electronic Engineering Technology, University of Johannesburg, Johannesburg 2028, South Africa
[3] Department of Electrical and Information Engineering, Covenant University, Ota, Ogun State, Nigeria
[4] HRA, Institute for Systems Science, Durban University of Technology, Durban, South Africa
Email: aitamakinde@abuad.edu.ng (A.A.I.); ejidokunto@abuad.edu.ng (T.O.E.);
adejumobibabatunde@gmail.com (B.S.A.); tshongwe@uj.ac.za (T.S.);
emmanuel.adetiba@covenantuniversity.edu.ng (E.A.); eowolabi2002@yahoo.com (I.E.O.)
*Corresponding author

***Abstract*—This paper presents the description, measurements, and analysis of an investigation into the path loss channel characteristics of a complex building environment using the College of Engineering building of Afe Babalola University, Ado-Ekiti, Nigeria as a case study. The study is conducted on the first floor of the building, which is compartmentalized into five scenarios. The measurements are performed in the distinctive line-of-sight and non-line-of-sight paths. Over 90% of the measurements taken are in the non-line-of-sight environment of the complex building. The wideband sliding correlator channel sounder measurement technique of 1.2 GHz centre frequency was performed using the National Instrument Universal Software Radio Peripheral (NI USRP) 2920/GNU (GNU's Not Unix) radio testbed. Key statistical considerations associated with path loss are calculated and the path loss equation model for the non-line-of-sight and line-of-sight of the entire first floor of the complex building is obtained. The results of the investigation show that an increase in path loss is a function of distance. The calculated path loss exponents were used to rate the performance of the wireless communication channel. The values obtained were found to be in tandem with the existing path loss metrics. Also, the radio propagation along the enclosed passages and indoor environments experienced low path loss, while the radio propagation along the ornamental trees encountered large path loss. Consequently, the results of the linear regression model and the log-normal model equation of Nonline of Sight (NLOS) and Line of Sight (LOS) results are somehow correlated. These results are useful in predicting the path loss of the radio signal at any specific distance from the transmitter to the receiver in any environment similar to the one under investigation. Also, as a planning and coverage optimization tool for wireless communication designers.**

***Keywords*—channel propagation, log-normal model, path loss, regression analysis, sliding correlator, software-defined radio, GNU radio**

I. Introduction

The wireless communication system has taken an essential role in technological development. Virtually every economic and human endeavour is now thriving based on the adoption of the wireless communication system [1]. The exponential increase in the wireless communication system is due to the ability of a single node of communication to connect wirelessly with billions of other nodes at the same time, in any part of the world, within a second [2]. Due to an increase in complex indoor/outdoor wireless radio communication system utilization, it is essential to investigate the channel characteristics of radio wave propagation in a complex building environment [3]. This will aid the proper modelling and design of the wireless communication system, giving good Quality of Service (QoS).

The complex nature of the building structure, the furniture, and the equipment layout in the rooms (such as the library, laboratory, staff room, lecture room, etc.) are the features that control the radio wave propagation in the complex building environment. These features produce the multipath effect, whereby several radio-wave signals are attenuated with different strengths at the receiver [4]. The wireless radio Path Loss (PL) propagation models are classic empirical mathematical expressions for the categorization of radio waves for the distance, frequency, and other factors that affect wireless radio signals in a specified transmission medium [5]. When deploying a wireless communication system to a specific environment with a peculiar landscape, obstacles, and weather conditions that depend on the propagation location, it is inappropriate to derive the same mathematical equation model for the entire scenario in the environment. Consequently, estimating the PL in different scenarios is expedient to effectively offset the loss of radio signals while transmitting the signal [6].

Manuscript received October 13, 2023; revised December 20, 2023; accepted December 26, 2023; published August 14 2024.

PL is said to be an anticipated loss of received power when the radio signal is sent from the Transmitter (Tx) to the Receiver (Rx) at a particular distance due to the properties of arbitrary large-scale fading. Losses due to the increase in radio propagation length, reflection, diffraction, penetration, and scattering are the main propagation problems [7]. Likewise, the density of building material, the building shape, and the building height cause the PL [8]. PL degrades the QoS of a wireless radio transmission, which most often leads to connection failure. Without a doubt, minimizing the influence of PL is the most important objective to accomplish in any wireless communication system [9]. In communication systems, several empirical PL mathematical equation models have been formulated to estimate the efficiency of the system and they are used extensively to forecast, plan, optimize, and simulate the radio signal strength between the Tx and Rx at a certain distance [10]. They are usually formulated from radio propagation channel measurements in practical user scenarios. The measurement data evaluated from the model parameters are accurate for only an actual frequency span environment and antenna positioning for the selected user scenario [7].

Empirical models are not the only existing models for predicting the received signal power level in wireless channel propagation. Other propagation models used are deterministic and semi-deterministic models [11, 12]. Empirical models are statistical and commonly used due to their simplicity, as they only require a few parameters, resulting in precise and concise equations. However, when applied to more universal environments, their precision may be insufficient [12, 13]. In deterministic models such as Ray tracing and Finite-difference-time-domain, the architectural plans and topography maps of the propagation channel environment are used to predict wave propagation characteristics. They provide comparatively accurate predictions but are not computationally efficient [14]. Recent research has used neural networks and other regression methods to predict path loss. Regression analysis is utilized to develop a one-slope log-distance model and to suggest a modified two-slope log-distance model for measuring path loss values [15]. The regression analysis successfully assists in the prediction of a path loss model in a different operating environment by using measurement data from a specific scenario [16].

The rest of the paper is organized as follows: Section II examines related works on path loss models in urban, suburban, and indoor environments. The technicality of the experimental setup at each measurement location or scenario, as well as the data processing and analysis used for the investigations, are discussed in Section III. The findings and a comprehensive discussion of the findings are presented in Section IV. While Section V contains the conclusion and recommendations for future works.

II. Literature Review

Several papers on PL measurements in both indoor and outdoor propagation have been published, including the Path Loss Exponent (PLE) of the environments, as reported in [17–20]. In Nigeria's environment, most of the publications on PL measurements were performed in urban or suburban environments only, and limited were done indoors.

Popoola [6] examined and built the PL propagation model for terrestrial radio transmission, broadcasting by Osun State Broadcast Corporation (OSBC) station in Ikire, Nigeria. The RSS in Ikire is measured with the BC1173 field strength metre. Several empirical models were employed and the results showed that the PL prediction approach used outperformed the COST-231 Hata model in the literature. The comparative performance analysis results show the need to develop different PL models for different radio signals in different situations under varied environmental conditions.

Akanni and Odepian [17] presented a comparative study of outdoor prediction models with measured data and channel power, using Ogbomoso, South-Western Nigeria, as the experimental campaign location. 150 MHz (VHF) and 900 MHz (UHF) frequency bands are used for the measurements. Free space, Okumura, and Egli propagation PL models are evaluated and correlated with the measured data. The results and statistical analysis indicated that the Okumura model agreed with the measured PL for the considered frequency bands, whereas free space and Egli overestimated the measured PL. The results also showed that the channel power decreases with an increase in distance.

Wassie *et al.* [20] proposed using wireless ultra-reliable communication in an industrial setting to replace wired connections for controlling critical processes. Based on measurements at 2.3 and 5.7 GHz, the study was carried out in complex industrial scenarios where the environments were practically overrun with large metallic machinery and concrete structures. When compared to a simple one-slope distance-dependent path loss model, the results showed that the convectional log-normal model is too simple for this environment. Furthermore, the results reveal that the PLEs in both scenarios are less than two in LOS, owing to the waveguiding effects of many reflections on various metallic machines. PLE values in NLOS are larger in dense factory clutter.

Ubom *et al.* [21] performed an indoor investigation of the throughput and attenuation effect on block walls of various sizes. InSSIDer software, laptops, a spectrum analyzer, and other pieces of measurement equipment were used in the experiments. The experiments were carried out in a lecture hall, an engineering drawing studio, and offices at Akwa Ibom State University in Nigeria. The results show that as block size increases, so does Wi-Fi signal attenuation. The results confirmed the previously established relationship between path loss and distance. Using the measured PL model to compare the free space, wall and floor factor, and ITU models received signal, the floor factor and ITU models clearly differed and were lower than the measured model, whereas the free space model is much higher.

Faruk *et al.* [22] developed a low-cost, time-efficient setup for measuring multi-transmitter path loss propagation in the VHF and UHF bands. The preserves shadowing effects and filtering algorithm were employed.

Several empirical and geospatial (Kriging) models were taken into account. However, when compared to Kriging, the Standard Deviation (SD) errors for all empirical models were low. This paper investigates the Kriging method's viability in predicting distance-based path losses in the VHF and UHF bands. This method was developed to reduce the cost of path loss measurements, analysis, and prediction in built-up propagation environments.

Using regression analysis, Zakaria *et al.* [23] developed propagation models in urban and suburban areas at an operating frequency of 3.5 GHz. To obtain the channel response, the measurements are carried out using a spectrum analyzer. According to the results, the PL could be calculated as a function of distance. Various measurements and calculated values of PLE at the urban and sub-urban levels were also analyzed and compared. Any radio will experience PL when travelling through a wireless propagation channel at a specific Tx-Rx distance.

Norberti *et al.* [24] used a deterministic, commercial Ray-Tracing (RT) software model to characterize the indoor-to-outdoor wireless propagation channel. The PL experience was quantified using RT simulation by a signal transmitted from random user terminals located inside a building to two Unmanned Aerial Vehicles (UAV) in two different locations for an emergency scenario. When PL models were compared to the RT software model, the PL models failed to fully capture the characteristics of the simulated environment. Actually, alternative UAV positions outside the building and the directional antenna were not considered, nor were realistic user distributions in emergency scenarios.

Hashir *et al.* [25] used USRP/LabVIEW software to investigate indoor channel characteristics based on a measurement campaign in an indoor environment. The measurements were taken on the second floor of a university building, and some existing models were examined, and their modelling accuracy was evaluated by comparing them to the measurement results. Unlike previous models, the authors' new proposed model took into account not only the effect of distance and walls on propagation loss but also the effect of glass doors and windows. When compared to previous models, the proposed method produced better results.

In this work, Software-Defined Radios (SDRs), the Universal Software Radio Peripherical (USRP)/GNU radio, are adopted for the measurement of the PL in a simple single-input and single-output (Tx-Rx) configuration, using the sliding correlator channel sounding technique at 1.2 GHz centre frequency. USRP/GNU radio provides the software used to define the radio and perform the output power measurements [26]. Subsequently, the measurements gathered from the measured environments are used to model the PL of the first floor of the Afe Babalola University Ado-Ekiti (ABUAD) College of Engineering (COE) first floor.

In other parts of the world, various researchers have investigated and determined path loss properties as well as appropriate statistical models within complex building environments. This study will add to the body of knowledge and improve the investigated area's Quality of Service (QoS).

III. The Experimental Setup for Path Loss Investigation

This chapter builds on the theoretical framework described in Chapter 2 and describes the experimental setup used to investigate path loss in a complex building environment, which is critical for validating the theoretical models. The experimental setup described in this chapter is designed to provide a practical and realistic setting for studying path loss in complex building scenarios, which is critical for developing accurate and dependable wireless communication systems.

A. Experimental Set-up

The radio strength measurement and hardware experimental requirements are NI USRPs/GNU radio, host computer, UPS, USB gigabit Ethernet adapter with RJ 45 cable, and VERT400 antennas. The setup for this work is shown in Fig. 1(a)–(c), consisting of the NI USRP whose band ranges from 50 MHz to 2.2 GHz, and the Omni-directional VERT400 tri-band (144 MHz, 400 MHz, 1200 MHz) antennas. The host computers used for the investigation are HP Pro 3520 all-in-one desktop computers, 64-bit processor, and RAM with an installed capacity of 6 GB and a dual-core Pentium processor that operates at a frequency of 3 GHz. The software setup requirement used in this experiment is GNU Radio, which is an open-source software.

An external USB gigabit ethernet (GbE) adapter and a 1-meter length Cat.5 cable are used to interface the USRP module to the host computer, at both the transmitter and receiver's side. The VERT400 antenna is fixed to the Tx1/Rx1 terminal of both Tx and Rx USRP. The Rx antenna acts as an output, while the Tx antenna acts as an input. The NI-USRP transmitter and receiver are placed at a different distance in each of the scenarios where the measurements are recorded. The Tx is placed 2.50 m above the floor and the receiver at 1.15 m above the floor.

TABLE I. Measurement Parameters

Parameter	Value	Note
Centre frequency	1.2 GHz	-
Sampling frequency	1.0 GHz	-
Transmitter antenna	VERT400 vertical antenna polarized, tri-band antenna.	Omni-directional vertical polarized antennas
Received antenna		
Tx antenna height	2.50 m	-
Rx antenna height	1.15 m	-
Transmitter power	8 dBw	-
Tx gain range	0 dB – 31 dB	-
Rx gain range	0 dB – 31.5 dB	-

The measurements are done by considering the line of sight (LOS) and Non-LOS (NLOS) between the Tx and Rx on the first floor of the COE building. The host PC is installed with GNU Radio software, which is used to implement SDR and other signal-processing systems. Measurement parameters for this work are presented in Table I.

TABLE I. MEASUREMENT PARAMETERS

Parameter	Value	Note
Centre frequency	1.2 GHz	–
Sampling frequency	1.0 GHz	–
Transmitter antenna	VERT400 vertical antenna polarized, tri-band antenna.	Omni-directional vertical polarized antennas
Received antenna		
Tx antenna height	2.50 m	–
Rx antenna height	1.15 m	–
Transmitter power	8 dBw	–
Tx gain range	0 dB – 31 dB	–
Rx gain range	0 dB – 31.5 dB	–

B. Measurement Locations and Scenarios

The investigation was performed on the first floor of the COE complex building of ABUAD and the building plan is shown in Fig. 2. During the measurement campaign planning, 27 data collection snapshots and 5 scenarios were considered. The first floor of the building has six wings (A, B, C, D, E, and F). The experiment environment has a lecture room, two libraries, offices, Laboratories (Lab), and Toilets (PTs).

The building rooms are majorly detached using plastered walls and painted ceramic boards, while glass framed with aluminium is used for windows. The doors are mostly wooden while the doors to the provost secretary's office (PSO), and library are made of aluminium sheets. The building floor's grounded finishing is ceramic tile and the balcony is safeguarded with iron barriers 1.10m high from the floor. A typical lecture room, library, laboratory, and Staff Office (SO) situated on the first floor of the building are shown in Fig. 2.

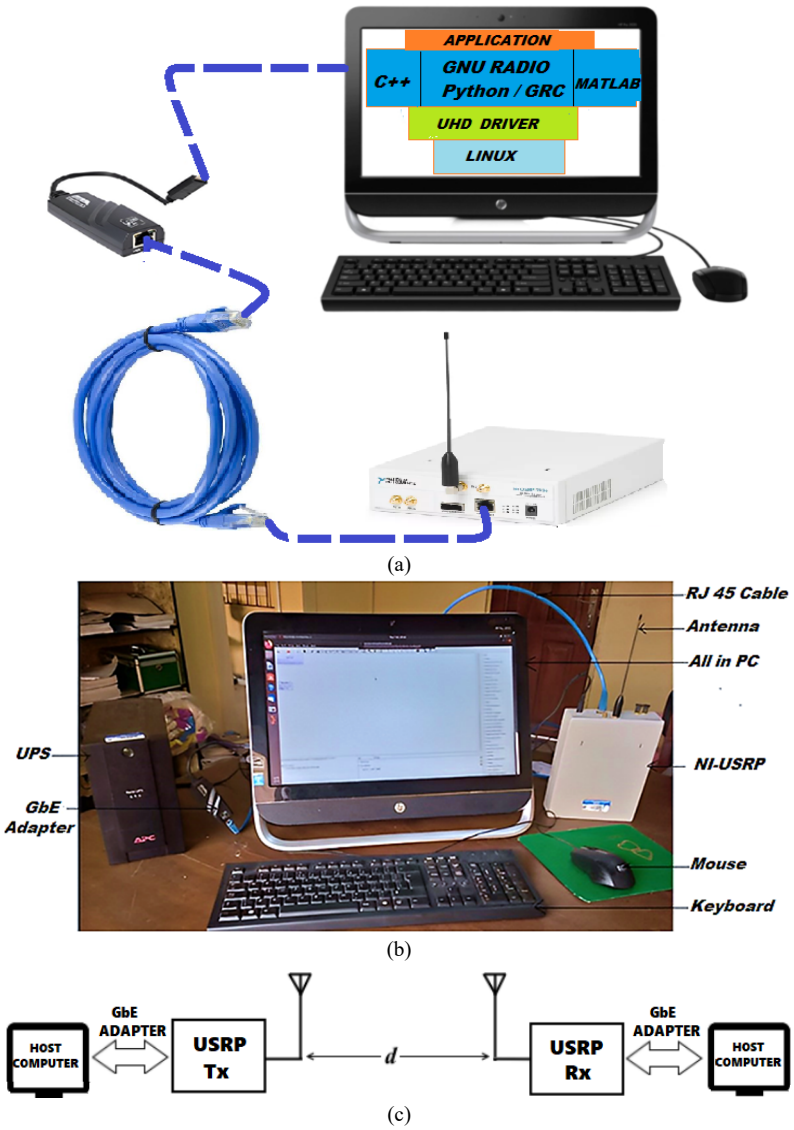

Fig. 1. System setup, (a) emulation, (b) picture, (c) The system SISO configuration.

During the investigation, three snapshots were taken at the same position within the lecture room on the first floor, situated on wing D. The first snapshot was taken when the room was emptied. The second was taken when people were moving randomly within the medium between Tx and Rx. And lastly, the third one was taken when the lecture room was filled with furniture. However, all other fixed or moveable objects within the measurement locations were left at their actual placement.

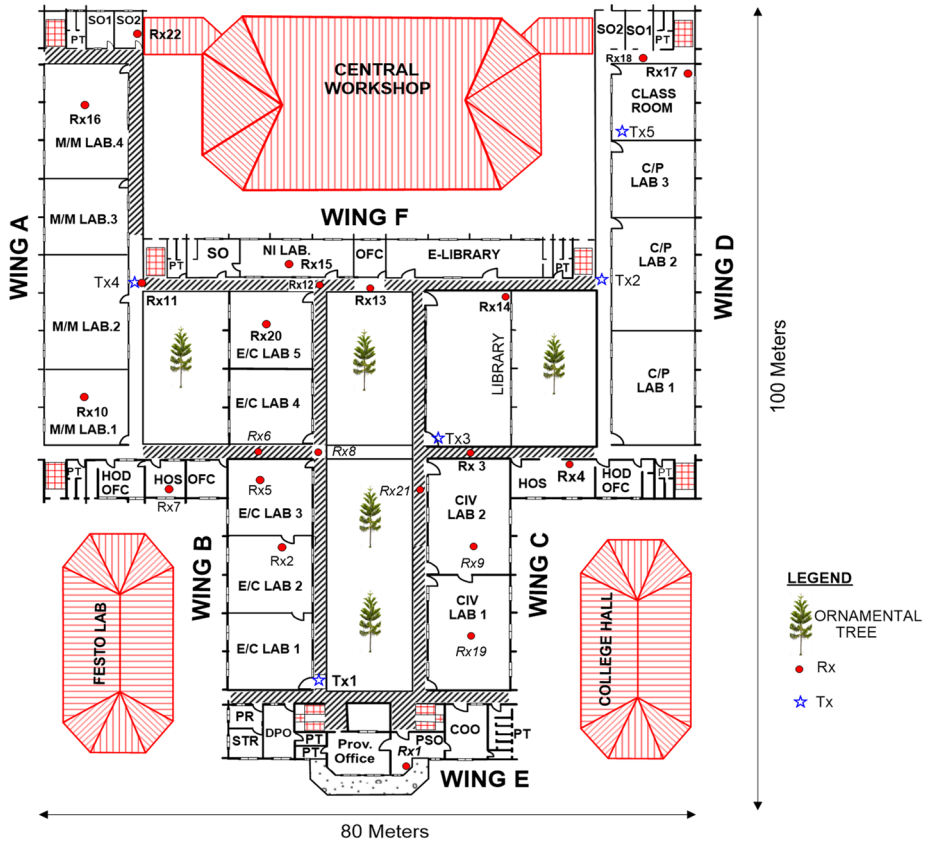

Fig. 2. ABUAD COE first floor Tx and Rx.

1) Scenario-1

The measurement was performed in this scenario by placing Tx1 beside the E/C Lab1 door entrance, situated on the balcony of wing B.

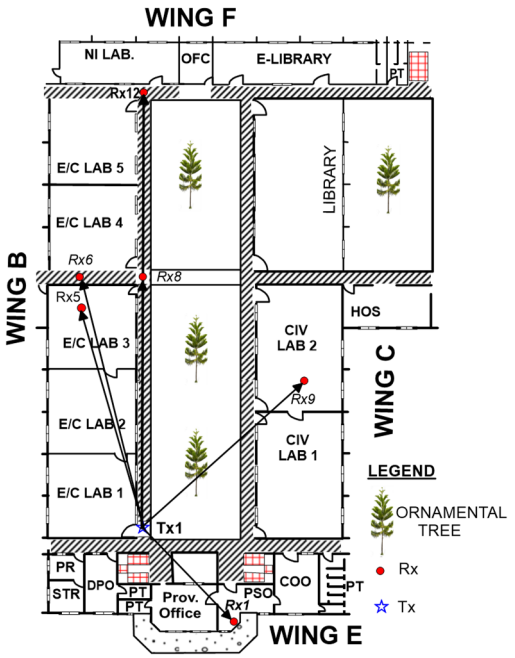

Fig. 3. Scenario-1 transmitter and six receivers' location plan.

The six receivers in this scenario are situated in different locations as indicated in Fig. 3. Rx1, Rx5, Rx6, and Rx9 are in NLOS, while Rx8 and Rx12 are in LOS environments as described in Table II, which also includes the distance between Tx1 and each of the six receivers in this scenario (see Table II).

TABLE II. SCENARIO-1 ENVIRONMENT

Tx	Rx	T-R Distance (m)	Environment	Comment
Tx1	1	15.00	NLOS	Windows closed, doors closed
Tx1	5	25.50	NLOS	Windows closed, entry door opened
Tx1	6	29.70	NLOS	–
Tx1	8	29.00	LOS	–
Tx1	9	25.00	NLOS	Windows closed, doors closed
Tx1	12	50.00	LOS	–

TABLE II. SCENARIO-1 ENVIRONMENT

Tx	Rx	T-R Distance (m)	Environment	Comment
Tx1	1	15.00	NLOS	Windows closed, doors closed
Tx1	5	25.50	NLOS	Windows closed, entry door opened
Tx1	6	29.70	NLOS	–
Tx1	8	29.00	LOS	–
Tx1	9	25.00	NLOS	Windows closed, doors closed
Tx1	12	50.00	LOS	–

2) Scenario-2

For this scenario, Tx2 is situated at the T-junction that connects the wing F passage with the balcony of wing D. Scenario-2 has five Rxs, four of the Rxs are in NLOS while one is in the LOS environment as shown in Fig. 4. Table III shows that two measurements were taken at Rx15, for when the door leading to the National Instrument (NI) laboratory is closed and opened, also the states of the doors and windows of Rxs positions and the distance between the Tx2 and Rxs are as well recorded (see Table III).

TABLE III. SCENARIO-2 ENVIRONMENT

Tx	Rx	T-R Distance(m)	Environment	Comment
Tx2	4	20.00	NLOS	Windows closed, doors closed
Tx2	5	46.00	NLOS	Windows closed, doors closed
Tx2	11	56.00	LOS	–
Tx2	15	38.50	NLOS	Windows closed, doors closed
Tx2	15	38.50	NLOS	Windows closed, doors opened
Tx2	21	34.00	NLOS	–

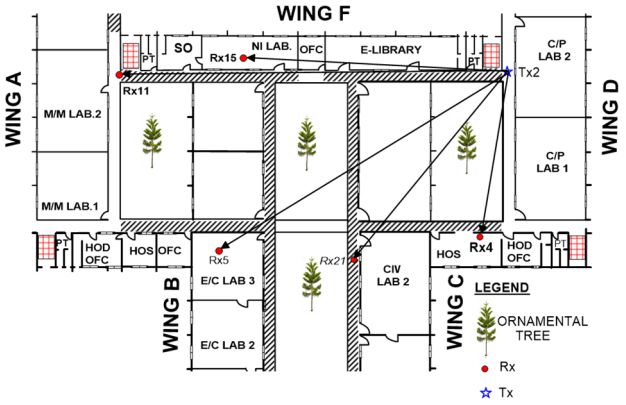

Fig. 4. Scenario-2 transmitter and four receivers' location plan.

3) Scenario-3

TABLE IV. SCENARIO-3 ENVIRONMENT

Tx	Rx	T-R Distance (m)	Environment	Comment
Tx3	2	24.00	NLOS	Windows closed, doors closed
Tx3	3	4.50	NLOS	Windows closed, doors opened
Tx3	13	21.30	NLOS	–
Tx3	14	19.70	NLOS	Windows closed, doors closed
Tx3	19	26.98	NLOS	Windows closed, doors closed

The Tx3 in scenario-3 was placed behind the library entrance door. The five Rxs are located in the NLOS environment as shown in Fig. 5. The distance between Tx3 and the five Rxs, the type of environments, and the states of doors and windows in each measurement taken are recorded in Table IV.

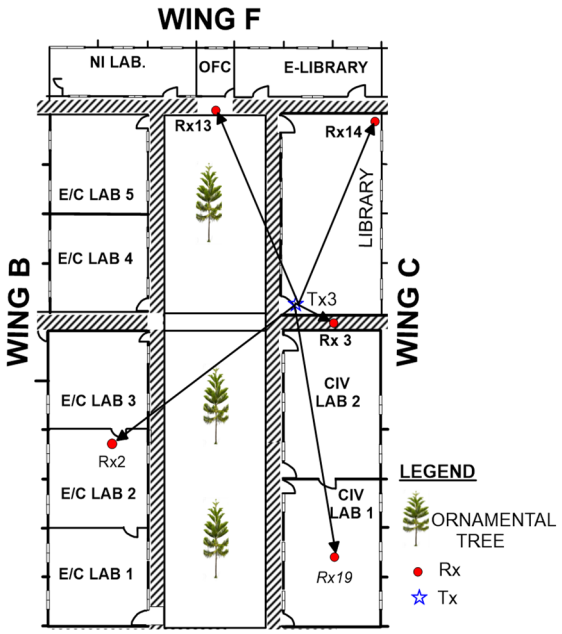

Fig. 5. Scenario-3 transmitter and five receivers' location plan.

4) Scenario-4

The Tx4 was placed at the T-junction of the block A passage adjoining the wing F balcony. Scenario-4 has five Rxs in NLOS environments as shown in Fig. 6. Table V states the measured distance between the Tx4 location and the respective locations of the Rxs, the specific location environment and the states of the doors and windows were also detailed.

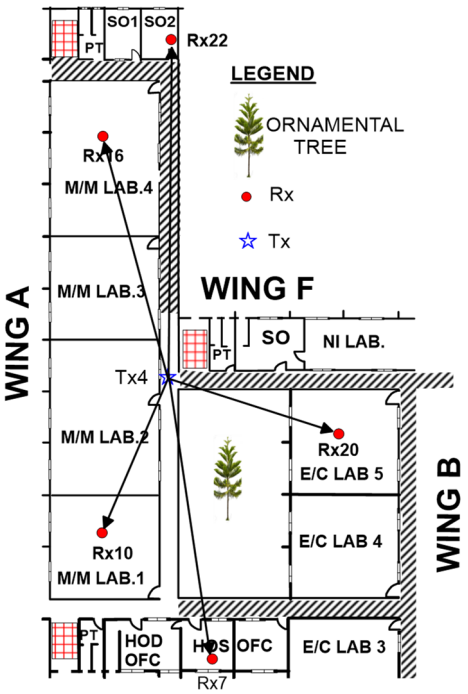

Fig. 6. Scenario-4 transmitter and five receiver's location plan.

TABLE V. SCENARIO-4 ENVIRONMENT

Tx	Rx	T-R Distance (m)	Environment	Comment
Tx4	7	26.90	NLOS	Windows closed, doors closed
Tx4	10	17.20	NLOS	Windows closed, doors closed
Tx4	16	25.30	NLOS	Windows closed, doors closed
Tx4	20	17.70	NLOS	Windows closed, doors opened
Tx4	22	33.00	NLOS	Windows closed, doors closed

5) Scenario-5

The Tx5 was located in a single lecture room in wing D on the first floor of the engineering college building. It was placed in the corner opposite the entrance of the lecture room. Four snapshots were taken in two Rxs (Rx17 and Rx18) positions. At location Rx17, three measurements were performed. The other measurement was performed at the Rx18 position, located outside the lecture room beside the staff office1 (SO1) window, on the passage as shown in Fig. 7. The Scenario-5 environments are presented in Table VI. Two measurements were collected at Rx17: one in an empty environment devoid of furniture, and another in which people were moving randomly between Tx5 and Rx17. And the last one was taken with well-arranged furniture in the lecture room. Similarly, the measured distance between Tx5 and the two Rxs (Rx17 and Rx18) locations, the environmental condition of the measurement area, and the situation of the doors and windows were recorded in Table VI.

TABLE VI. SCENARIO-5 ENVIRONMENT

Tx	Rx	T-R Distance (m)	nvironment	Comment
Tx5	17	11.80	LOS	Empty classroom. Windows closed, doors opened
Tx5	17	11.80	NLOS	Lecture room with furniture. Windows closed, doors opened
Tx5	17	11.80	NLOS	The random movement of people within the Tx and Rx in the classroom. The door opened; the widow closed
Tx5	18	10.20	NLOS	Windows closed, doors opened

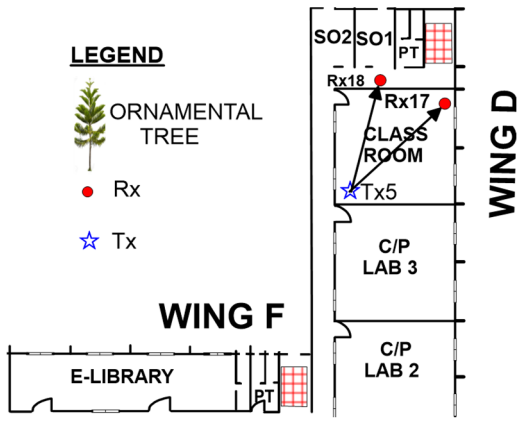

Fig. 7. Scenario-5 transmitter and two receivers' location plan.

C. Data Processing and Analysis

This work evaluates and models the PL of the wireless radio propagation channel of the investigated complex building environment. It employs the log-normal shadowing path loss model. The log-normal distribution is said to be arbitrary shadowing effects obtained from an extensive number of measurement areas that have the same distance between Tx and Rx, but not the same level of clutter on the propagation channel's path [18]. In log-normal shadowing model estimation, the independent variables, usually on the x-axis, need to be considered to predict and understand the expression of the dependent variables, usually on the y-axis [18].

The Matlab software tool is used for data analysis and allows the estimation of parameters of the log-normal shadowing regression model such as standard deviation, path loss exponent, adjusted regression slope, coefficient of determination (r^2), and coefficient of multiple correlations (r). The Received Signal Power (RSP) values, obtained from the measured locations on the first floor of the COE complex building were changed to the values of PL. Typically, the formula that relates the PL received power and transmitted power is stated in Eq. (1) [27]:

$$PL(S)[dB] = P_t\,[dBm] - P_r[dBm] + G_t[dB] + G_r[dB] \quad (1)$$

where, $PL(S)$ is the path loss at distance S, P_t indicates transmitted power, P_r is the received power, G_t indicates transmit antenna gain, while G_r is the receive antenna gain.

Moreover, in the free space model, as the influence of the earth is disregarded, it is anticipated that there is a perfect LOS pathway between the Tx and Rx. The free space path loss equation model is expressed as Eq. (2) [28].

$$PL(S)[dB] = 10log\frac{P_t}{P_r} = -10log\left(\frac{\lambda^2}{(4\pi)^2 S^2}\right) \quad (2)$$

where, $PL[S]$ is the path loss and, S is the distance between Tx and Rx, while λ is the wavelength gotten from the frequency at which the system communicates.

When a distribution is log-normal, it is known as log-normal shadowing. Having the same distance in an irregular environmental clutter at various locations is not observed for only log-distance. This causes the measured radio signals to be largely distinct from the predicted average value by the log-distance PL model [18]. To justify these irregularities, a more accurate generic equation that models the effect of PL shadowing is expressed in Eq. (3) [29], for the average PL ($PL(S)$) and distance (S) from Tx and Rx:

$$PL(S) = \overline{PL}(S) + Z_\sigma \quad (3)$$

where, $\overline{PL}(S)$ is the received power calculated at each Tx-Rx separation distance (estimated power) and Z_σ is the zero mean arbitrary variables with normal distribution and SD (σ) The estimated received power is solved by using Eq. (4) [30].

$$\overline{PL}(S) = PL(S_0) + 10\times\rho\times log\left(\frac{S}{S_0}\right)\ \ S \geq S_0, \quad (4)$$

where, as Eq. (2) is a free space propagation model equation and its distance (S_0) is the reference distance from the transmitter (Tx-Rx separation distance). To estimate the PLE (ρ) and σ, Eqs. (5–7) are adopted. Eq. (5) [30] can be used to evaluate the ρ by reducing the Mean Square Error (MSE) of the estimated received power.

$$e(\rho) = \sum_{i=1}^{k} ([PL(S) - \overline{PL}(S)])^2 \quad (5)$$

where, k is the number of distances measured between Tx and Rx. When equating the derivatives of Eq. (5) to zero as in Eq. (6) [30], the value of the quantity of ρ, can be solved.

$$MSE = \frac{\partial}{\partial \rho} e(\rho) = 0 \quad (6)$$

The result obtained can be used to solve the σ of the channel. Let us define Eq. (5) as the total sum of variation between the received power and the estimated power. Therefore, σ is expressed in Eq. (7) [30] as:

$$\sigma = \sqrt{\frac{e(\rho)}{N}} \quad (7)$$

where, N is the number of samples.

TABLE VII. PATH LOSS EXPONENT FOR DIFFERENT ENVIRONMENTS

Environment	Path Loss Exponent (ρ)
Free Space	2
Urban area cellular radio	2.7 to 3.5
Shadowed urban cellular radio	3 to 5
In building line-of-sight	1.6 to 1.8
Obstructed in buildings	4 to 6
Obstructed in factories	2 to 3

However, depending on the environment, ρ and σ vary from one scenario to the other. Table VII indicates ρ of different environments [17, 30].

For a coefficient of determination (r), it is described as a rate of deviation of the dependent (or response) variable that can be clarified by the independent (or explanatory) variable [31]. The mathematical formulation used to evaluate r^2 is expressed in Eq. (8) [32]:

$$r^2 = 1 - \frac{\sum_{n-1}^{n} (y_n - \hat{y}_n)^2}{\sum_{n-1}^{n} (y_n - \bar{y}_n)^2} \quad (8)$$

where, $\bar{y} = \frac{1}{n} \sum_{n=1}^{n} y_n$, $\hat{y}$ is the prediction value, while y_n is the measured path loss value.

The coefficient of multiple correlations in this perspective provides measured data corresponding to the rate of a dependent variable and an array of independent variables. It is expressed in Eq. (9) [31, 32] as

$$r = \sqrt{r^2} \quad (9)$$

Suitably, when adjusting a log-normal shadowing model, it is essential that the r^2 and r have values that are greater than 0.7. If the value of r^2 is equal to 1, it shows that there is a perfect connection between the variables. Also, if the r^2 is less than 0.3, it shows that there is no relationship between the variables [33].

IV. RESULTS AND DISCUSSION

The measurements were performed in each of the scenarios to study the behaviour of the received signal attenuated power. Table VIII shows the regression analysis for the predicted PL for the measured environment. The sum of the polynomial equation for the LOS equation in serial numbers 5, 19, 26, 27 and NLOS equations in other serial numbers is $3093 - 3356.16\rho + 922.87\rho^2$ and $68741 - 32820.04\rho + 3954.42\rho^2$, respectively. The polynomial mathematical equation or MSE equation, by equating the derivative of the polynomial equation to zero as in Eq. (5), is used to evaluate the predictive PL model. Table 9 also indicates the distance between Tx and Rx, the type and number of partitions, the received signal strength, the estimated path loss exponent (ρ), and the standard deviation (σ) in each of the scenarios. In addition, the formulated path loss models are presented and discussed in this section, and the regression plots also called a line of best fit of scatter plots, are plotted as shown in Figs. 8–12.

TABLE VIII. REGRESSION ANALYSIS TABLE

S/N	S(m)	Pr(dBm)	PL(dB)	$\overline{PL}$ (dB)	PL - $\overline{PL}$	(PL − $\overline{PL}$) ^{2}
1.	1.00	−26	34.00	34.00	0	0
2.	4.50	–50	58.00	34.00+ 6.53ρ	24 - 6.53ρ	$576 - 313.44\rho + 42.64\rho^2$
3.	10.20	–66	74.00	34.00+10.09ρ	40 - 10.09ρ	$1600 - 807.20\rho + 101.81\rho^2$
4.	15.00	–66	74.00	34.00+ 10.41ρ	40 - 10.41ρ	$1600 - 832.80\rho + 108.37\rho^2$
5.	11.80	–40	48.00	34.00+ 10.72ρ	14 - 10.72ρ	$196 - 300.16\rho + 114.92\rho^2$
6.	11.80	–63	71.00	34.00+ 10.72ρ	37 - 10.72ρ	$1369 - 793.28\rho + 114.92\rho^2$
7.	11.80	–67	75.00	34.00+ 10.72ρ	41 - 10.72ρ	$1681 - 879.04\rho + 114.92\rho^2$
8.	17.20	–76	84.00	34.00+ 12.36ρ	50 - 12.36ρ	$2500 - 1236\rho + 152.77\rho^2$
9.	17.70	–67	75.00	34.00+ 12.48ρ	41 - 12.48ρ	$1681 - 1023.36\rho + 155.75\rho^2$
10.	19.70	–71	79.00	34.00+ 12.94ρ	45 - 12.94ρ	$2025 - 1164.60\rho + 167.44\rho^2$
11.	20.00	–77	85.00	34.00+ 13.01ρ	51 - 13.01ρ	$2601 - 1327.02\rho + 169.26\rho^2$
12.	21.30	−80	88.00	34.00+ 13.28ρ	54 - 13.28ρ	$2916 - 1434.24\rho + 176.36\rho^2$
13.	24.00	–85	93.00	34.00+ 13.80ρ	59 - 13.80ρ	$3481 - 1628.40\rho + 190.44\rho^2$
14.	25.00	–87	95.00	34.00+ 13.98ρ	61 - 13.98ρ	$3721 - 1705.56\rho + 195.44\rho^2$

15.	25.30	–89	97.00	34.00+ 14.03ρ	63 - 14.03ρ	$3969 - 1767.78\rho + 196.84\rho^2$
16.	25.50	–92	100.00	34.00+ 14.07ρ	66 - 14.07ρ	$4356 - 1857.24\rho + 197.96\rho^2$
17.	26.90	–88	96.00	34.00+ 14.30ρ	62 - 14.30ρ	$3844 - 1773.20\rho + 204.49\rho^2$
18	26.98	–91	99.00	34.00+ 14.31ρ	65 - 14.31ρ	$4225 - 1860.30n + 204.78\rho^2$
19.	29.00	–55	58.00	34.00+ 14.62ρ	24 - 14.62ρ	$578 - 701.76\rho + 213.74\rho^2$
20.	29.50	–97	105.00	34.00+ 14.70ρ	71 - 14.70ρ	$5041 - 2087.40\rho + 216.09\rho^2$
21.	33.00	–86	94.00	34.00+ 15.19ρ	60 - 15.19ρ	$3600 - 1822.80\rho + 230.74\rho^2$
22.	34.00	–95	103.00	34.00+ 15.31ρ	69 - 15.31ρ	$4761 - 2112.78\rho + 234.40\rho^2$
23.	38.50	–86	94.00	34.00+ 15.85ρ	60 - 15.85ρ	$3600 - 1902\rho + 251.22\rho^2$
24.	38.50	–89	97.00	34.00+ 15.85ρ	63 - 15.85ρ	$3969 - 1997.10\rho + 251.22\rho^2$
25.	46.00	–101	109.00	34.00+ 16.63ρ	75 - 16.63ρ	$5625 - 2494.50\rho + 276.56\rho^2$
26.	50.00	–56	64.00	34.00+ 16.99ρ	30 - 16.99ρ	$900 - 1019.40\rho + 288.66\rho^2$
27.	56.00	–60	68.00	34.00+ 17.48ρ	34 - 17.48ρ	$1156 - 1188.64\rho + 305.55\rho^2$
		Total (e(ρ))				$71834 - 36176.20\rho + 4877.2\rho^2$

The scenario-1 result shown in Table IX reveals that there is a significant difference in ρ values between the LOS (free space) and NLOS. The ρ values estimated for Rx8 (ρ = 1.98) and Rx12 (ρ = 1.77) from the Tx1 location are within the range of ρ of free space as indicated in Table 7, so also the partitioned environments, which indicate relatively lossy environments (ρ = from 3.84 to 4.83). Table 9 also indicates that there are more path losses experienced in the NLOS environment (for Rx1, Rx5, Rx6, Rx9) than in LOS (for Rx8, Rx12), and there is a wide variation in signal attenuation between the NLOS and LOS.

The difference between the highest NLOS and the lowest LOS is 42 dB. This is attributed to the density of the barrier such as the glass window, walls, and ceramics partition between the transmitter and receivers. In the two LOSs (Rx8 and Rx12) in this scenario, the PL of Rx12 (64 dB) is slightly higher than Rx8 (58 dB) and it is expected that the Rx12 should be much higher when compared with its distance from Rx8 to Tx1. Rx12 is slightly higher due to its closeness to the reflective wall, unlike Rx8. Furthermore, σ which is 19.09 dB, is higher due to the substantial distinction caused by the wide variation between ρ values of various types of radio propagation environments. Fig. 8 indicates the scenario-1 path loss scatter (regression) plot.

In scenario-2, as presented in Table IX, two snapshots were taken in the Rx15 environment, when the door was opened and closed. The PL and ρ of these two states are estimated and compared. The results showed a difference of 3 dB and 0.18, respectively, indicating that the state of the door (opened or closed) has little or no effect on the propagated signals. Likewise, the PL estimated for the two states at Rx15 has 94 dB and 97 dB for the opened and closed doors respectively.

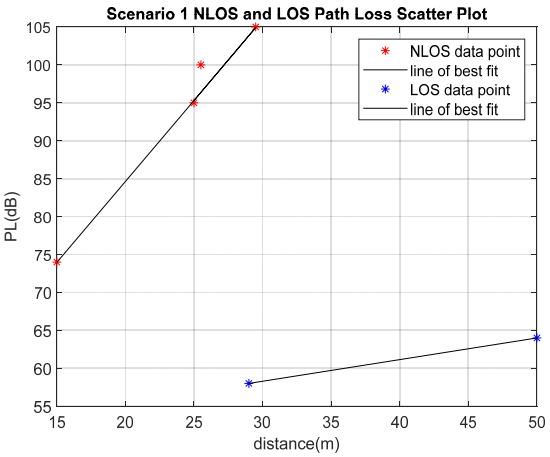

Fig. 8. Scenario-1 regression plot.

TABLE IX. THE REVIEW OF SCENARIO-1 TO SCENARIO-5 CHANNEL PROPAGATION MEASUREMENT

	Rx	T-R (m)	Partition	#	PL (dB)	ρ	σ (dB)
			SCENARIO-1				
Tx1	1	15.00	Ceramic board	1			
			Glass window	1	74	3.84	
Tx1	5	25.50	Plaster wall	1			
			Ceramic board	2	100	4.69	
			Glass window	1			
Tx1	6	29.50	Plaster wall	2			19.09
			Ceramic board	2	105	4.83	
			Glass window	1			
Tx1	8	29.00	LOS	–	58	1.98	
Tx1	9	25.00	Plaster wall	2	95	4.36	
			Wooden door	1			
Tx1	12	50.00	LOS	–	64	1.77	
			SCENARIO-2				
Tx2	4	20.00	Plaster wall	1	85	3.92	
Tx2	5	46.00	Plaster wall	3	109	4.51	
Tx2	11	56.00	LOS	–	68	1.95	14.74
Tx2	15	38.50	Plaster wall	3	94	3.79	
			Door Opened	–			
Tx2	15	38.50	Plaster wall	3	97	3.97	

			Door closed	1			
Tx2	21	34.00	Plaster wall	3	103	4.51	
			SCENARIO-3				
Tx3	2	24.00	Plaster wall	2	93	4.28	4.87
			Ceramic board	1			
Tx3	3	4.50	Plaster wall	1	58	3.68	
Tx3	13	21.30	Plaster wall	1	88	4.07	
Tx3	14	19.70	Library	–	79	3.48	
Tx3	19	26.98	Plaster wall	2	99	4.54	
			SCENARIO-4				
Tx4	7	26.90	Plaster wall	1	96	4.34	5.45
Tx4	10	17.20	Plaster wall	1	84	4.05	
			Ceramic board	1			
Tx4	22	33.00	Wooden door	1	94	3.95	
Tx4	16	25.30	Plaster wall	1	97	4.49	
			Ceramic board	1			
Tx4	20	17.70	Glass window	1	75	3.29	
			SCENARIO-5				
Tx5	17	11.80	Empty classroom (LOS)	–	48	1.31	11.41
Tx5	17	11.80	Classroom furniture	–	71	3.45	
Tx5	17	11.80	12 people moving randomly	–	75	3.82	
Tx5	18	10.20	Plaster wall	1	74	3.96	

Furthermore, when these estimated values are compared with PL of Rx21 (103 dB) at a lesser distance and the same number of partitions, it is observed that a few meters of enclosed passage along the radio path from Tx2 to Rx15 and the enclosed location of Rx15 acted as a waveguide. This makes the PL at the Rx15 location to be lesser. Likewise, the enclosed passage along the Rx11 location reduces Rx11 path loss. Consequently, the standard deviation (14 dB) obtained in this scenario is due to a 31 dB attenuation difference between only LOS and the highest NLOS conditions. In this scenario, the σ is lesser when compared to scenario-1, this is due to the lesser deep variation between ρ of Rx at NLOS and LOS locations. The PL regression plot of scenario-2 is shown in Fig. 9.

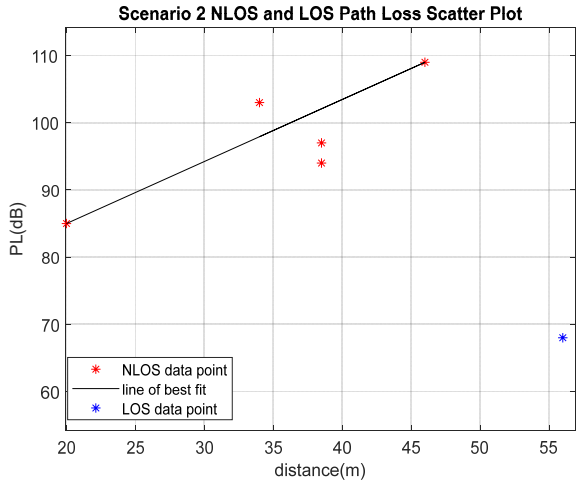

Fig. 9. Scenario-2 regression plot.

Scenario-3 generally indicates that there is a relative reduction in path loss, ρ, and standard deviation (5.64 dB) when compared with the two prior scenarios. This is attributed to the shorter distances, relatively lower partition density, three out of five measurements taken in enclosed environments, and the nonavailability of the LOS environment between Tx and Rx in scenario-3. This enclosed room acts as a waveguide which causes constructive interference. Scenario-3 scatter plot is shown in Fig. 10.

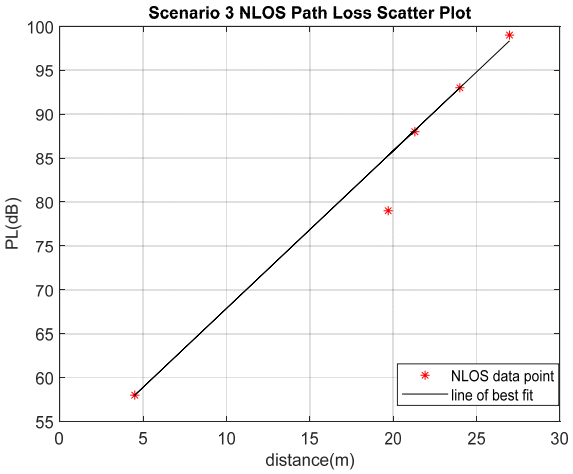

Fig. 10. Scenario-3 regression plot.

The estimated PL (4.09) and overall σ (5.45 dB) obtained for scenario-4 are very close to the outcome in scenario-3. The drastic reduction in the computed value in scenarios-3 and 4 is due to the LOS condition not being considered in these scenarios, as indicated in Table IX.

It is a clear indication that an increase in the number of partitions between Tx and Rx yields a corresponding increase in the path loss. Fig. 11 shows the log-distance model scatter plot for scenario-4.

In scenario-5, three major cases were investigated at the Rx17 position; the empty classroom, the random movement of people between Tx and Rx, and the classroom filled with furniture. The results are shown in Table IX, as expected, the empty classroom (LOS) exhibits the lowest path loss and ρ when compared with the other cases. This is due to the LOS condition in the empty classroom. A comparison of the signal response at Rx18 with the other three cases at Rx17 shows that the path loss at Rx18 and the second case at Rx17 were almost the same, with a difference of just 1 dB.

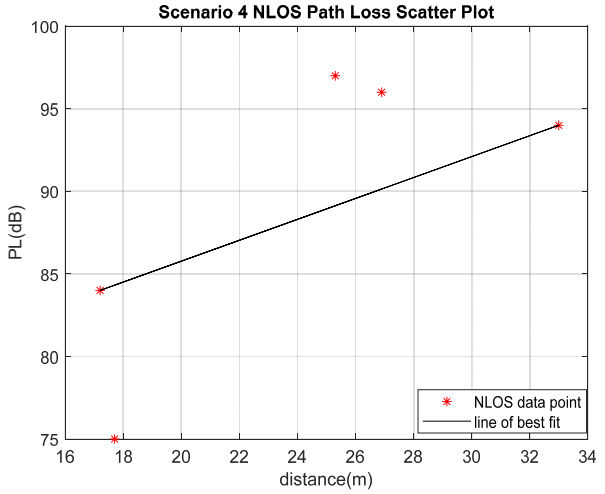

Fig. 11. Scenario-4 regression plot.

The outcome demonstrates that the plastered wall, which is a significant barrier between Tx5 and Rx18 creates shadow fading and increases path loss. Also, the estimation of the indoor-to-outdoor path loss is marginally greater when compared with the indoor environment estimation. The σ in this scenario is higher when compared to scenario-3 and 4, this is due to the presence of LOS. The lower LOS path loss estimate increases the value of the standard deviation. Scenario-5 path loss scatter plot is shown in Fig. 12.

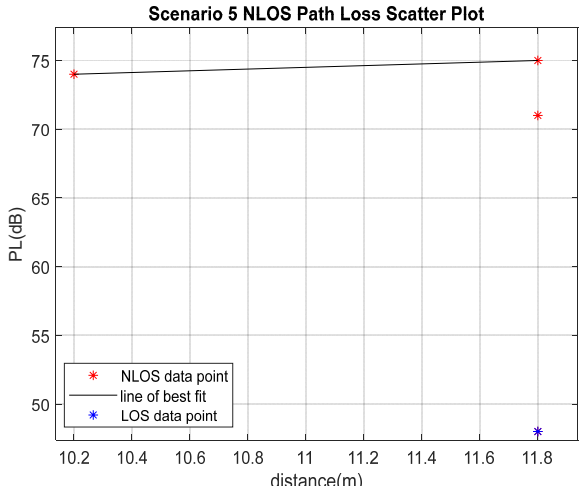

Fig. 12. Scenario-5 regression plot.

Considering the PL model of the entire measured area, ρ and σ are estimated using regression analysis with MATLAB (V.R2019a) with the composite data of all five scenarios for the linear regression plots.

The LOS and NLOS linear plots are plotted on a single plot as shown in Fig. 13. The NLOS ρ and σ values, 4.15 and 5.41 dB respectively are estimated using Eqs. (5–6). Likewise, the LOS ρ value, 1.82, and σ value, 2.89 dB are obtained.

Essentially, a linear regression plot is generally employed as a method of predictive analysis in wireless communication. It can be used to assess the correlation between two or more disparate data by drawing a line of best fit to derive a linear equation. The equation model for a linear regression plot is given as $y = A + Bx$, where x denotes the explanatory variable and y is the response variable [22].

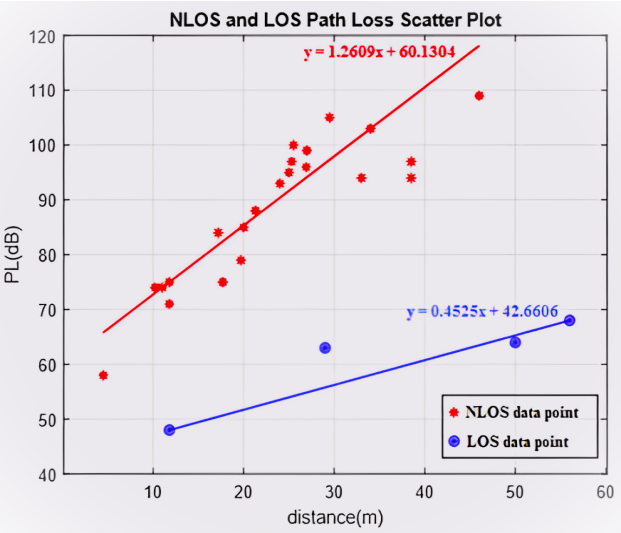

Fig. 13. Log-normal shadowing regression line model for NLOS and LOS.

Consequently, for NLOS and LOS of the whole first floor, the linear regression equation gives the coefficient of determination (r^2) as 0.79 while the coefficient of multiple correlations (r) is 0.89. These values are higher than 0.7, as discussed in the last paragraph of subsection C, under Section III. The NLOS linear regression equation of the line of the best fit is expressed as in Eq. (10).

$$y = 1.2609\,x + 60.1304 \quad \text{or}$$
$$PL(dB) = 1.2609\,S(m) + 60.1304 \tag{10}$$

where S is the distance in metres.

For LOS, the coefficient of determination (r^2) is 0.82 while the coefficient of multiple correlations (r) is 0.91; also, these values are higher than 0.7 and the linear regression equation related to the best of line fit is expressed as in Eq. (11):

$$y = 0.4525\,x + 42.6606 \quad \text{or}$$
$$PL(dB) = 0.4525\,S(m) + 42.6606 \tag{11}$$

when PL is expressed in the form of Eqs. (3)–(4), the log-normal model reflects the ρ, and the following Eqs. (12–13) are obtained for NLOS and LOS respectively.

$$PL(dB) = 34 + 4.15 \times (10)\,log(S) + Z_{5.41} \tag{12}$$

$$PL(dB) = 34 + 1.82 \times (10)\,log(S) + Z_{2.89} \tag{13}$$

where $\rho = 4.15$ and $\sigma = 5.41$ dB for Eq. (12), and $\rho = 1.82$, and $\sigma = 2.89$ dB for Eq. (13). In both cases, $PL(S_0) = 34$ dB is the PL associated with the reference distance, S_0, from the transmitter.

Log-normal and regression models are the two statistical models used in this work. The application choices between them in the real world have practical implications. The coefficients in a linear regression model show the predictor's additive influence. Every unit change in the predictor results in a constant change in the outcome. In a log-normal model, the coefficients denote relative effects. A percentage change in the result is caused by a unit change in the predictor [34]. Linear regression is based on the assumption that residuals are normally distributed and have a constant variance. If these data assumptions are met, a log-normal model may be more appropriate [35]. Log-normal can help make data more "normal" or symmetric, meet the constant variance assumption, and make a non-linear relationship more linear [34].

However, if the relationship is linear and the sample size is large (less than 100), using the maximum likelihood method to estimate absolute effects in a log-normal model yields unbiased point estimates and accurate coverage for both confidence and predictor intervals. When the relationship is linear, however, using log transformation (which is commonly used for regression on log-normal data) can result in erroneous point estimates, liberal prediction intervals, and erroneous confidence intervals [36]. A linear regression model would be more appropriate if the outcome variable can take any value on the real line (including negative values). If your outcome variable is strictly positive, a log-normal model may be more appropriate [37].

However, there are significant drawbacks to this study that may restrict its generalizability to other complex structures. The constraints of this experiment are the building's structure, the ornamental trees planted in an unenclosed quadrangle within the building, and the density of the obstacles within the propagation channels. Thus, the results may not be relevant to buildings with varying structures and higher barrier densities. The study only analysed five scenarios on the first floor of the building's five floors. Limited scenarios and other floors were not explored, which may limit the results' applicability. The research was carried out with specialised equipment (NI USRP 2920 modules and GNU radio software). The frequency range of this device is 50 MHz to 2.2 GHz. If a higher frequency or other equipment is utilised, the results may differ.

V. Conclusion

This study presents an empirical wireless propagation channel model for 1.2 GHz transmission on the first floor of the ABUAD College of Engineering building. The findings are critical for understanding radio signal power loss and its thresholds, aiding in the design of wireless communication systems to enhance Quality of Service (QoS).

The log-normal shadowing Path Loss (PL) method was used due to its ease of execution and the environment's complexity, with regression analysis validating the log-normal equation. PL propagation measurements were conducted using the National Instruments (NI) USRP module, an all-in-one desktop computer, and an omnidirectional antenna. The study found that PL, ρ, and σ values vary due to differences in obstruction density between the transmitter (Tx) and receiver (Rx).

Regression analysis helped analyze the relationship between explanatory and response variables. The PL linear regression equations for Non-Line-of-Sight (NLOS) and Line-of-Sight (LOS) scenarios were compared with those derived from the log-normal shadowing model, showing correlated values. In NLOS environments, obstructions like furniture, walls, and moving people cause path loss and signal attenuation. Structural materials and objects within the propagation channel also contribute to path loss. Techniques such as beamforming, MIMO systems, rotating antennas, diversity, equalization, and error coding can mitigate these issues.

The study evaluated and used log-normal and linear regression equations to predict path loss. Linear regression predicts signal strength at specific distances from the transmitter, aiding in strategic transmitter placement for optimal coverage. The log-normal equation is useful where network phenomena follow a log-normal distribution, providing accurate signal behaviour predictions in complex environments. Machine learning approaches are increasingly combined with these mathematical tools to enhance channel modelling and estimation.

Key results include (a) Linear regression model, (i) for NLOS: PL(dB) = 1.26 S(m) + 60.134, and (ii) for LOS: PL(dB) = 0.45 S(m) + 42.66, where S(m) is the distance between Tx and Rx. (b) Log-normal model, (i) for NLOS: $PL(dB) = 34 + 4.15(10)\times\log(S) + Z_{5.41}$, with $\rho = 4.15$ and $\sigma = 5.41$ (ii) for LOS: $PL(dB) = 34 + 1.82(10)\times\log(S) + Z_{2.89}$, with $\rho = 1.82$ and $\sigma = 2.89$. PL is 34 dB for both models, representing the reference distance S from the transmitter.

Future work includes implementing fixed MIMO channel measurements and investigating propagation channels during high-traffic periods. Movement in the wireless communication channel causes signal variation due to Doppler shift shadowing and multipath fading, more pronounced during rush hour, leading to significant changes in signal interference.

Employing millimeter-wave (mmWave) frequencies (6 GHz and above) can provide higher bandwidth and data rates, faster and more reliable wireless communication, and reduced interference through beamforming techniques. However, mmWave frequencies face challenges such as increased propagation loss, penetration loss, and sensitivity to blocking and mobility. The choice of frequency band significantly impacts path loss and wireless communication system performance in complex building environments.

Conflict of Interest

The authors declare no conflict of interest.

Author Contributions

A.A. Itamakinde conceptualized, experimented, and wrote the manuscript. T.O. Ejidokun reviewed and edited

the manuscript, while B.S. Adejumobi and Thokozani Shongwe also reviewed, analyzed the data, and processed the Article Processing Charges (APCs). I.E. Owolabi and E. Adetiba supervised the work. All authors had approved the final version.

FUNDING

This research APC was funded by the University of Johannesburg, Johannesburg, South Africa

REFERENCES

[1] B. J. Folayan and M. K. Obun-Andy, "Impact of social media on the socio-economic development of Nigeria," *Impact of social media on the Socio-Economic Development of Nigeria*, vol. 3, 2020, pp. 1–14.

[2] A. Tanweer, "Efficient and secure data transmission approach in cloud-MANET-IoT integrated framework," *Tanweer Alam. Efficient and Secure Data Transmission Approach in Cloud-MANET-IoT Integrated Framework, Journal of Telecommunication, Electronic and Computer Engineering*, vol. 12, no. 1, 2020.

[3] M. Dangana *et al*., "Towards the digital twin (DT) of narrow-band internet of things (NBIoT) wireless communication in an industrial indoor environment," *Sensors*, vol. 22, no. 23, 2022.

[4] M. Hervás, P. Bergadà, and R. M. A. Pagès, "Ionospheric narrowband and wideband HF soundings for communications purposes: a review," *Sensors,* vol. 20, no. 9, 2020, p. 2486.

[5] A. Alhamou *et al*., "Empirical investigation of the effect of the door's state on received signal strength in indoor environments at 2.4 GHz," in *Proc. 39th Annual IEEE Conference on Local Computer Networks Workshops*, IEEE, 2014, pp. 652–657.

[6] J. J. Popoola, "Assessment and development of path loss propagation model for Ikire metropolis, Nigeria," *Aksaray University Journal of Science and Engineering*, vol. 5, no. 1, 2021, pp. 20 – 35.

[7] C. Gustafson, T. Abbas, D. Bolin, and F. Tufvesson, "Statistical modelling and estimation of censored path loss data," *IEEE Wireless Communications Letters,* vol. 4, no. 5, 2015, pp. 569–572.

[8] G. R. Maurya, P. A. Kokate, S. K. Lokhande, and J. A. Shrawankar, "A review on investigation and assessment of path loss models in urban and rural environment," in *Proc. IOP Conference Series:* Materials *Science and Engineering*, vol. 225, no. 1, 2017, p. 012219.

[9] C. Pradhan and G. R. Murthy, "Analysis of path loss mitigation through dynamic spectrum access: Software defined radio," in *Proc. 2015 International Conference on Microwave, Optical and Communication Engineering (ICMOCE)*. IEEE, 2015, pp. 110 – 113.

[10] Z. E. Khaled, W. Ajib, and H. Mcheick, "An accurate empirical path loss model for heterogeneous fixed wireless networks below 5.8 GHz frequencies," *IEEE Access,* vol. 8, 2020, pp. 182755 – 182775.

[11] S. Cheerla, D. V. Ratnam, an H. S. Borra, "Neural network-based path loss model for cellular mobile networks at 800 and 1800 MHz bands," *AEU-International Journal of Electronics and Communications,* vol. 94, 2018, pp. 179 – 186

[12] A. A. Itamakinde, T. O. Ejidokun, E. I. Owolabi, O. P. Awe, and B. S. Adejumobi, "Investigation of small-scale and multipath fading of radio wave propagation in a complex building environment," *International Journal on Communications Antenna and Propagation (IRECAP)*, vol 12, no. 6, pp. 411 – 427, 2022.

[13] Y. Zhang, J. Wen, G. Yang, Z. He, and J. Wang, "Path loss prediction based on machine learning: Principle, method, and data expansion," *Applied Sciences,* vol. 9, no. 9, 2019, p. 1908.

[14] L. Wu, D. He, B. Ai, J. Wang, H. Qi, K. Guan, and Z. Zhong, "Artificial neural network-based path loss prediction for wireless communication network," *IEEE Access,* vol. 8, 2020, pp. 199523 – 199538.

[15] Z. Gao, W. Li, Y. Zhu, Y. Tian, F. Pang, W. Cao, and J. Ni, "Wireless channel propagation characteristics and modelling research in rice field sensor networks," *Sensors*, vol. 18, no. 9, 2018, p. 3116.

[16] S. Aldossari and K. C. Chen, "Predicting the path loss of wireless channel models using machine learning techniques in mm-wave urban communications," in *Proc. 2019 22nd International Symposium on Wireless Personal Multimedia Communications (WPMC)*, vol. 1, 2019.

[17] A. O. Akanni and K. Odepian, "Comparative analysis of propagation path loss and channel power of VHF and UHF wireless signals in urban environment," *Int. J. Res. Innov. Appl. Sci*, pp. 1–6, 2019.

[18] R. Akl, D. Tummala, and X. Li, "Indoor propagation modeling at 2.4 GHz for IEEE 802.11 networks," *Wireless and optical communications*, pp. 12–17, 2006.

[19] S. Kaddouri, M. El Hajj, G. Zaharia, and G. E. Zein, "Indoor path loss measurements and modelling in an open-space office at 2.4 GHz and 5.8 GHz in the presence of people," in *Proc. 2018 IEEE 29th Annual International Symposium on Personal, Indoor, and Mobile Radio Communications (PIMRC)*, IEEE, 2018, pp. 1–7.

[20] D. A. Wassie, I. Rodriguez, G. Berardinelli, F. M. Tavares, T. B. Sorensen, and P. Mogensen, "Radio propagation analysis of industrial scenarios within the context of ultra-reliable communication," in *Proc. 2018 IEEE 87th Vehicular Technology Conference (VTC Spring)*, IEEE, 2018, pp. 1–6.

[21] E. A. Ubom, A. C. Akpanobong, and I. I. Abraham, "Characterization of indoor propagation properties and performance evaluation for 2.4 Ghz band Wi-Fi," *Available at SSRN 3391700*, p. 12, 2019.

[22] N. Faruk *et al*., "Large-scale radio propagation path loss measurements and predictions in the VHF and UHF bands," *Heliyon*, vol. 7, no. 6, 2021.

[23] Y. A. Zakaria, E. K. Hamad, A. S. A. Elhamid, and K. M. E. Khatib, "Developed channel propagation model and path loss measurements for wireless communication systems using regression analysis techniques," *Bulletin of the National Research Centre*, vol. 45, no. 1, pp. 1–11.

[24] L. Norberti, R. Nebuloni, and M. Magarini, "Characterization of the indoor-to-outdoor wireless channel in air-to-ground communication systems," in *Proc. 2020 16th International Conference on Wireless and Mobile Computing, Networking and Communications (WiMob)*, pp. 1–6, 2020, October.

[25] S. M. Hashir, S. Erkucuk, and T. Baykas, "A novel indoor channel model for TVWS communications based on measurements," in *Proc 2018 IEEE Conference on Standards for Communications and Networking (CSCN)*, 2018, October). pp. 1–6.

[26] R. Zitouni and L. George, "Output power analysis of a software-defined radio device," in *Proc. 2016 IEEE Radio and Antenna Days of the Indian Ocean (RADIO)*, 2016, October, pp. 1–2.

[27] A. Alsayyari, I. Kostanic, C. E. Otero, and A. Aldosary, "An empirical path loss model for wireless sensor network deployment in a dense tree environment," in *Proc. 2017, IEEE Sensors Applications Symposium (SAS)*, pp. 1–6, 2017.

[28] H. A. Hashim, S. L. Mohammed, and S. K. Gharghan, "Path loss model-based PSO for accurate distance estimation in indoor environments," J. Commun., vol. 13, no. 12, pp. 712–722.

[29] C. U. Kumari, P. Kora, K. Meenakshi, and K. Swaraja, "Short-term and long-term path loss estimation in urban, suburban, and rural areas," in *Proc. 2019, 3rd International Conference on Computing Methodologies and Communication (ICCMC)*, pp. 114–117, 2019.

[30] R. Desimone, B. M. Brito, and J. Baston, "Model of indoor signal propagation using Log-normal shadowing," in *Proc. 2015 Long Island Systems, Applications and Technology*, pp. 1–4, 2015, May.

[31] F. C. Vesga, H. M. F. Contreras, and B. J. A. Vesga, "Design of empirical propagation models supported by the Log-Normal Shadowing model for the 2.4 GHz and 5GHz bands under Indoor environments," *Indian J. Sci. Technol*, vol. 11, no. 22, pp. 1–18, 2018.

[32] H. S. Jo, C. Park, E. Lee, H. K. Choi, and J. Park, "Path loss prediction based on machine learning techniques: Principal component analysis, artificial neural network, and Gaussian process," *Sensors*, vol. 20, no. 7, p. 1927, 2020.

[33] D. Mindrila and P. Balentyne, "Scatterplots and correlation," *Retrieved From*, pp. 1–14, 2017.

[34] S. Gustavsson, *Evaluation of Regression Methods for Log-normal Data*, pp. 1–63, 2015.

[35] G. Vallet and M. Jose, "Characterization of the log-normal model for received signal strength measurements in real wireless sensor networks," *Journal of Sensor and Actuator Networks*, 2020, p. 12.

[36] A. R Villadsen and N. W. Jesper, "Statistical myths about log-transformed dependent variables and how to better estimate exponential models," *British Journal of Management*, 2021, pp. 779–796.
[37] C. Chatfield, "Introduction to multivariate analysis," *Mathematics and Statistics*, p. 24, 2018.